We are IntechOpen,
the world's leading publisher of
Open Access books
Built by scientists, for scientists

6,900
Open access books available

186,000
International authors and editors

200M
Downloads

154
Countries delivered to

Our authors are among the

TOP 1%
most cited scientists

12.2%
Contributors from top 500 universities

CLARIVATE ANALYTICS
BOOK CITATION INDEX
INDEXED

WEB OF SCIENCE™

Selection of our books indexed in the Book Citation Index
in Web of Science™ Core Collection (BKCI)

Interested in publishing with us?
Contact book.department@intechopen.com

Numbers displayed above are based on latest data collected.
For more information visit www.intechopen.com

From Tilings to Fibers – Bio-mathematical Aspects of Fold Plasticity

C. Lesieur and L. Vuillon

Additional information is available at the end of the chapter

1. Introduction

Protein oligomers are made by the association of protein chains via intermolecular amino acid interactions (interaction between subunits) forming so called protein interfaces. This chapter proposes mathematical concepts to investigate the shape constraints on the protein interfaces in order to promote oligomerization. First, we focus on tiling the plane (2 dimensions) by translation with abstract shapes. Using the fundamental Theorem of Beauquier-Nivat, we show that the shapes of the tiles must be either like a square or like a hexagon to tile the whole plane. Second, we look in more details at the tiling of a cylinder and discuss its relevancy in constructing protein fibers. The universality of such "building" properties are investigated through biological examples. This chapter is written four-hand by a mathematician and a biologist in order to present bio-mathematical aspects of fiber constructions.

Proteins are made by polymerization of 20 different amino acids via a covalent bond called the peptide bond. The ordered amino acids read along the peptide bonds constitute the protein backbone and are referred to as the primary structure or the primary sequence. The secondary structure involves hydrogen bonding to form α-helix or pleated-sheet structures. The intricate folding of the polypeptide chain in a globular protein via long range atomic interactions is referred to as the tertiary structure. Some proteins (hemoglobin, for example) have quaternary structure— several polypeptide chains are nested together. These proteins are called protein oligomers. The different chains associate by the formation of contact zones called protein interfaces, made of contacts between atoms of the amino acids (Fig. 1A). The majority of proteins are organized as oligomers and not as single monomers (for a review see chapter in this book by Gotte). Protein oligomers adopt different symmetries and different stoichiometries (number of repeated monomers). According to the PDB (Protein Data Bank [30]) where all available atomic structures of proteins are stored, protein oligomers exist in cyclic, dihedral and cubic point group symmetries. Most proteins have C_n or D_n symmetry (see [17, 22, 24]) and almost only viral proteins adopt cubic symmetry [35]. High stoichiometry complexes in eukaryotes have most often a C_1 symmetry (identity). Some proteins adopt helical symmetry and construct fibers (see [24]).

In this chapter, we investigate the construction of biological fibers by using a mathematical model for fibers. Essentially the formation of the fiber is considered as the tiling of an infinite height cylinder derived from an initial two dimensional tiling of the plane followed by the translation of a single tile. This single tile could be replaced by a n-mer in order to construct more complex fibers. Of course proteins have tridimensional shapes (3D-structure) and the biological fiber could have cross section and more complex internal organization not considered here because the idea is to construct a complete mathematical model for fibers applicable for any 3D-structure of the protein. This "simplification" is supported biologically because there exists many severe human diseases associated with the formation of fibers by proteins structurally and functionally unrelated. Notorious examples, are Alzheimer ($A\beta$-amyloid), Parkinson (synuclein), cerebral amyloid angiopathy (cystatin C-amyloidosis) and type II diabetes (IAPP, amylin). It is important to realize that fiber formation is also observed in cancer (p53), cardiovascular (transthyretin, serpin) and inflammatory diseases (serpin) (reviewed in [2, 6, 9, 26, 27]). These proteins (indicated in bracket next to the disease) have the fold plasticity to undergo a transition from an oligomeric state to a fiber state, change that leads to the loss of the protein function and the pathologies, called conformational diseases (Fig. 1B). Because this transition is shared by unrelated proteins, it is reasonable to assume that the change is based on a generic binding properties of the interface. The idea of the work is to define the shape constraints of the interfaces of a fiber (infinite height cylinder) compared to the interfaces of an oligomer (finite height cylinder) to ultimately address the problem of conformational diseases. The 2D tiling is relevant as the answer lies in the properties of surfaces. As mentioned, we are particularly interested in determining invariant properties, i.e. property of the surface that are true for any 3D-structure of the protein. In other words, the goal is to trace the local properties (the interface) necessary to carry out a global change. The relation between local properties and quaternary structures is discussed in details in the work by Claverie, Hofunung and Monod and the Monod, Changeux, Wyman (MCW) model ([8, 28]).

Clearly the transition to a fiber involves other determinants besides those of the protein interface, as for example the spatial positioning of the interface relative to the main body of the protein, a typical folding problem for which 3D-tiling would be more appropriate. Nevertheless this problem is not addressed in the present chapter which focus essentially on the transition from an oligomer to a fiber seen from the protein interface view point. For more information on the mechanisms of assembly and 3D determinant, one can read the chapter by Claire Lesieur titled "The Assembly of Protein Oligomers: Old Stories and New Perspectives with Graph Theory". For fiber formation, readers can referred to the work by Gebauer [11, 12].

This chapter proposes a mathematical approach of the problem using the principles of tiling and considering the protein interfaces as boundaries of a tile. The chapter is divided into 9 parts: (1) After this introduction. (2) We focus on usual C_n and D_n symmetries that build finite height cylinders and we explain the construction of interfaces between chains. In paragraph (3) we give a formal description of the boundary of a tile by using abstract geometrical objects called polyominoes, we state the fundamental Theorem of Beauquier-Nivat which explains the properties of the boundary of a tile associated with its capacity to tile a plan. (4) We present the regular tilings of the plane which are tilings constructed by translation of all integral combinations of 2 vectors. (5.1) These two directions of periodicity on the tilings allow us to construct fibers (that are infinite cylinders) and to
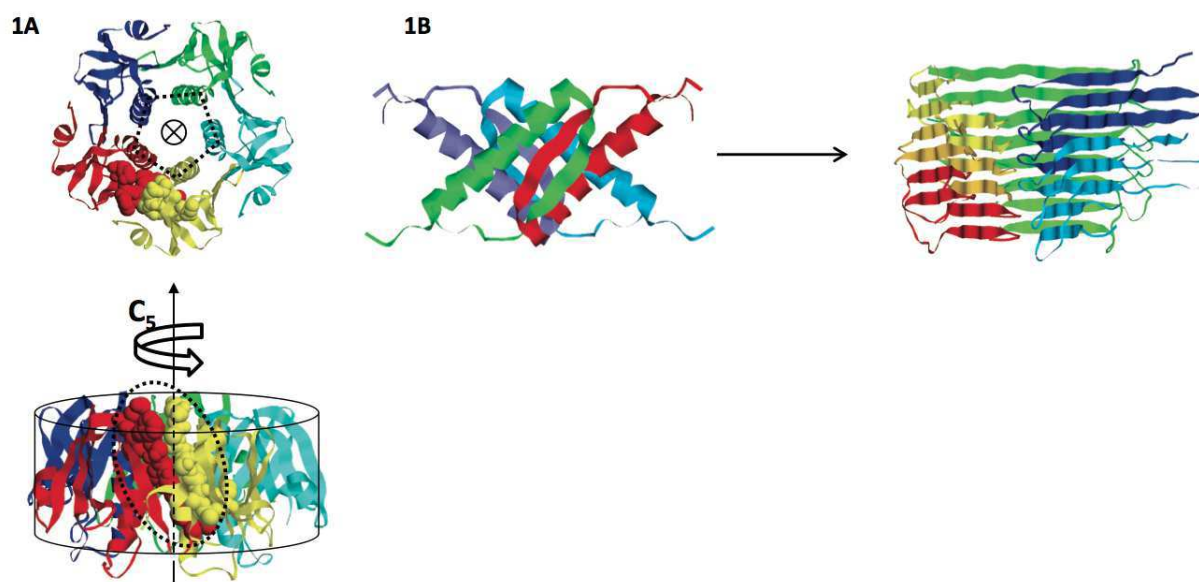
Figure 1. Protein oligomers and fibers. A. Protein oligomer. As an example, the x-ray structure of the cholera toxin B pentamer ($CtxB_5$) is shown (PDB code 3CHB). Each chain is indicated in a different ribbon color. The top and bottom images represent a top view and a side view of the pentamer, respectively. The atomic interactions involved in a protein interface are highlighted in space fill representation showing all atoms. Each chain participates for one domain of the interface, also called segment or side. ($CtxB_5$) has a C_5 symmetry that is well described by a cylinder (bottom image). **B. Oligomer to fiber transition.** Each monomer is indicated by a different color.

impose the use of either 2 interfaces or 3 interfaces. (5.2) We extend our construction to tile the fiber by n-mers instead of a single chain. (5.3) We explain how the fold plasticity is able to make a transition from finite cylinder to fiber in the p53 case. (6.1) We investigate the case of non regular tilings in order to design fibers with only 1 direction of periodicity and this implies strong constraints on the shape of the tile. (6.2) We also investigate transition from fiber to tiling of the whole three dimensional space. (7) We give a conclusion by comparing the fiber case to the whole tiling of the 3D space. All along this chapter biological illustrations are presented in parallel to the mathematical descriptions.

2. C_n and D_n symmetries on oligomerization

Oligomers with C_n symmetry can be constructed using a single chain replicated with a rotational axe of order n that is by a rotation of angle $360/n$ degrees (in other terms n equals to the number of monomers in the oligomers). Such oligomer adopts a cylindrical surface with each chain associating with 2 adjacent chains via a single interface (Fig. 1A). The interface is made of 2 interacting domains also called segments or sides, each one provided by one chain (Fig. 1A). It is important to clearly distinguish the notion of having one interface from the notion of having multiple regions or multiple patches of interfaces. Interfaces can be made of amino acids that are not contiguous along the backbone making up several "regions" (Fig. 2A). Yet the different regions still constitute a single interface because they are only able to bind to a single side. As an analogy, let's consider a poster to be stuck on a wall. You may choose to put several patches of glue on the reverse side of the poster or only one : it will

still bind to only one surface. The C_n oligomers have only 1 interface and they polymerize following a single direction that is why they can describe a cylindrical surface (fig. 1A). An important notion is the number of adjacent chains in the oligomerization. In the C_n symmetry, each chain has exactly 2 adjacent chains (namely the Mth chain has for adjacent chains the $(M-1)$th chain and the $(M+1)$th chain (this calculation is done modulo n)) (see fig. 3). To summarize C_n is an oligomerization with 1 interface (possibly with distinct regions) and with 2 adjacent chains at each chain (see Fig. 3 and Fig. 4).
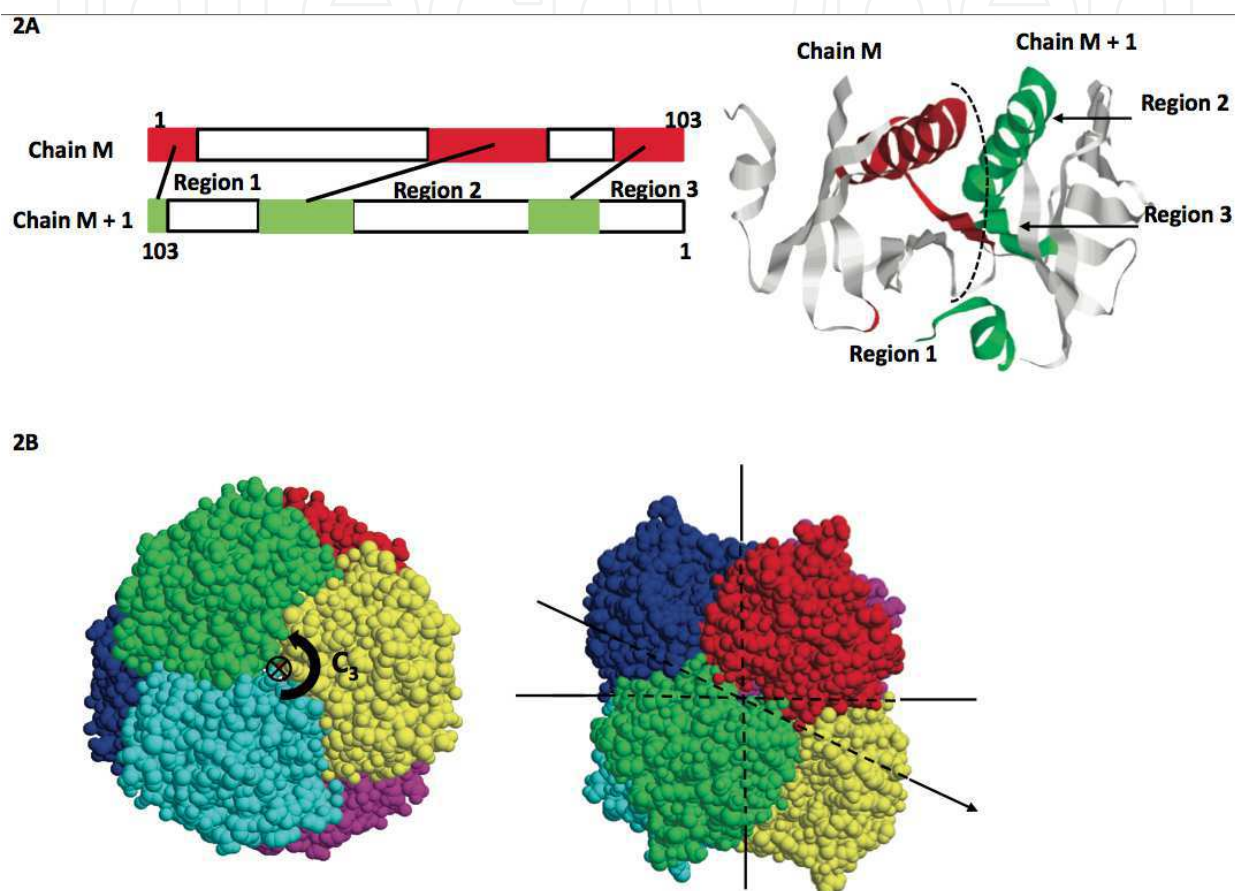
Figure 2. Protein interfaces. A. Left, rectangular schematic of the backbone of a protein oligomer. Two interacting chains are indicated, chain M and $M+1$. Chain M participates in one side of the interface indicated by the red boxes and chain $M+1$ participates in the complementary sides indicated in green. In the example the protein has 3 distinct regions of interface. Right, Illustration of the 3 regions of interface on the x-ray structure of CtxB5 (see fig. 1A). **B. D_n symmetry oligomer.** Example with the protein 3GVF (PDB code), a D_3 symmetry oligomer made of 6 chains organized as 3 dimers.

A slightly more complicated symmetry is the D_n symmetry oligomer which is reconstructed by a rotational axe plus 2 axes of symmetry perpendicular to the rotational axe. Such symmetry might look like to polymerize in 2 directions because it has one region of interface orthogonal to another one so the former can bind in a perpendicular direction. However, the "orthogonal" interface cannot grow besides forming a dimer so a D_n symmetry is in fact similar to a C_n symmetry considering the polymerization of a dimer instead of a monomer (Fig. 2B).
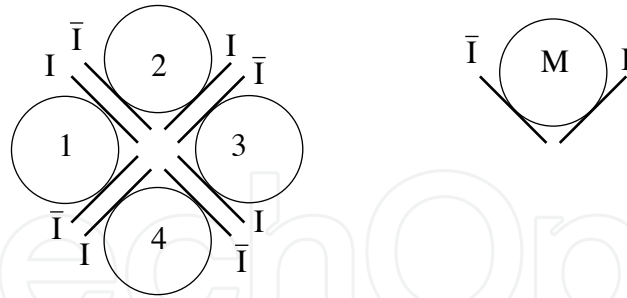
Figure 3. Abstract view of C_4 symmetry. A tetramer formed by a single interface between the part I and $\bar{I}$. Each chain is adjacent via the interface to exactly 2 other chains
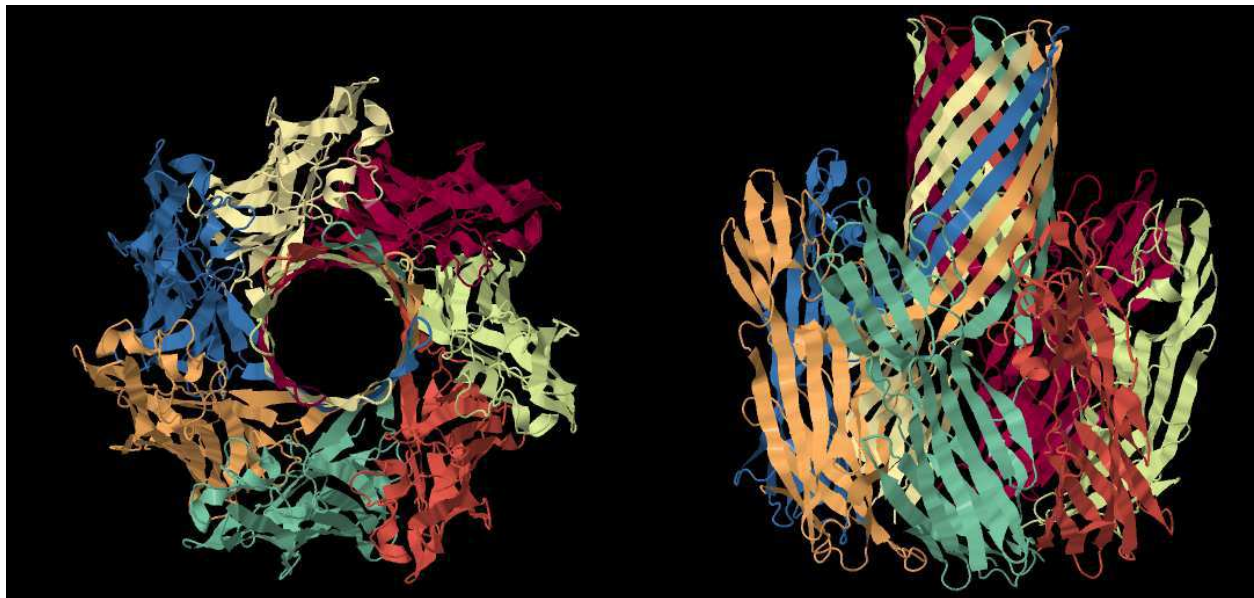

Figure 4. Heptamer with 4H56 PDB code with each chain adjacent to 2 other chains. Remark that in the beta barrel the adjacency between pairs of chains is the same as in the other part of the heptamer. This implies an oligomerization with exactly 1 interface.

3. Definitions and notation

A *polyomino* is a fundamental object in theory of tilings introduced by Golomb [16]. Polyominoes are building blocks for tiling and will be for us an abstract version of a single chain in an oligomerization process.

A polyomino is composed of juxtaposition of unit squares with corners on the $\mathbb{Z}^2$ grid (the corners of each unit square are integer points) such that every 2 adjacent squares in the polyomino share a unit segment; and also such that we can reach every pair of squares of the polyomino by a path inside the polyomino moving by unitary steps on adjacent unit squares (see Fig. 5).

The most simple polyomino has only one unit square and is called "mino"(Fig. 6).

There are 2 distinct polyominoes constructed by 2 adjacent unit squares and are called "domino". Remark that a domino can be horizontal or vertical this is why we find 2 dominoes (Fig. 7).
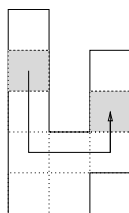
Figure 5. Path inside a polyomino

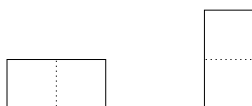**Figure 6.** The most simple polyomino: the mino

Figure 7. The 2 dominoes

There are 6 polyominoes constructed by 3 2-by-2 adjacent unit squares: an horizontal bar of 3 unit squares, a vertical bar of 3 unit squares and four "triominoes *L*" with 3 adjacent unit squares that form an "*L*" shape and the 3 rotations by 90, 180 and 270 degrees (Fig. 8).
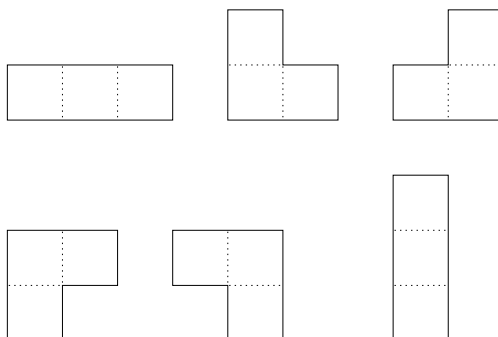

Figure 8. The 6 triominoes

In fact, the number of polyominoes with four unit squares (namely the tetraminoes) is 19.

In addition, the usual definition adds that there is no hole in the interior of a polyomino (Fig. 9).
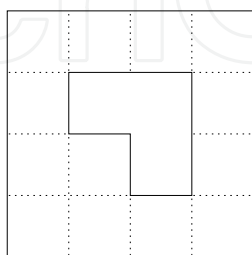

Figure 9. Union of unit squares with a hole in the interior

The number of polyominoes with *n* unit squares is given by the sequence number A001168 according to the Sloane Integer Sequences Encyclopedia (http://oeis.org/A001168): 1, 2, 6, 19, 63, 216, 760, 2725, 9910, 36446, 135268, 505861, 1903890, 7204874, 27394666,

104592937, 400795844, 1540820542, 5940738676, 22964779660, 88983512783, 345532572678, 1344372335524, 5239988770268, 20457802016011, 79992676367108, 313224032098244, 1228088671826973, ... We recognize the beginning of the sequence namely 1 mino, 2 dominoes, 6 triominoes, 19 tetraminoes and so on.

We don't know if it possible to find a closed formula (i.e. a mathematical formula depending on n that counts the number of distinct polyominoes with n unit squares) and this is a research problem for combinatorists.

We have defined polyominoes and now we would like to tile the whole plane by translation of a single polyomino.

Let P be a polyomino. A *tiling by translation* of P is a covering of the whole plane $\mathbb{R}^2$ by translated images of P such that there is no hole in the tiling and no overlapping. A polyomino that tiles the plane by translation is called a *tile* (Fig. 10).
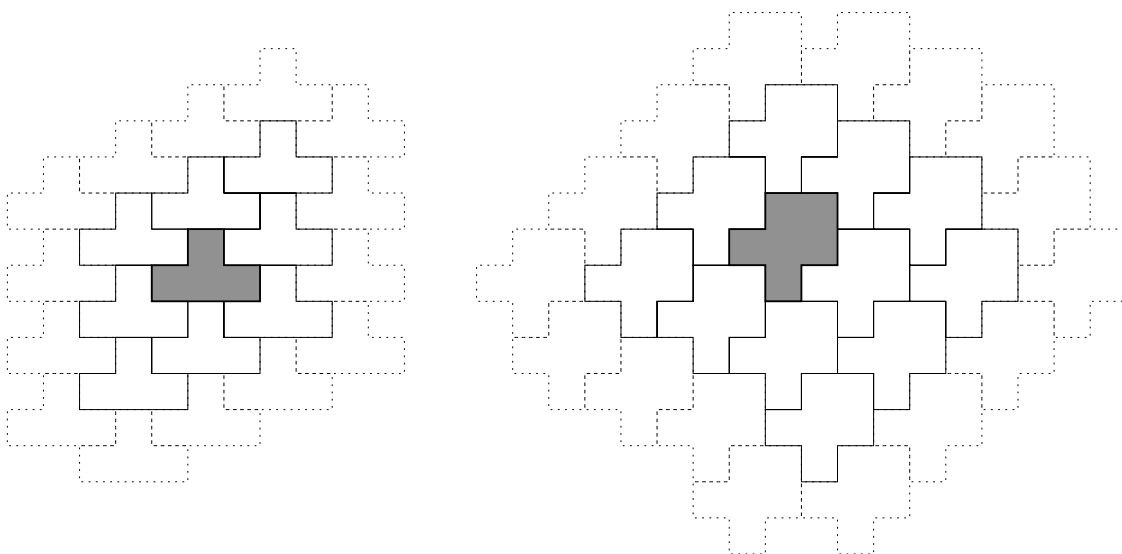

Figure 10. Tilings of the plane

Remark, that we use only translated images of P and neither rotation nor reflection nor glide reflection.

In order to find a characterization of polyominoes that tile the plane by translation we focus on the boundary of a polyomino P. We code the paths of the boundary by 4 letters: a represents a left step, b an up step, $\bar{a}$ a right step and $\bar{b}$ a down step.

Now, we take a starting point o on the boundary and we turn clockwise considering the sequence of steps in order to make a path constituted by unit segments from o to the first return on o. Let $\mathbf{b}(P)$ be a *boundary word of P* that is the path from o to o in clockwise that codes the boundary of the polyomino P in the following way : starting from an origin on the boundary o, the boundary word $\mathbf{b}(P)$ is the concatenation of labels of boundary unit segments read clockwise. Remark that as we turn clockwise we can't have in the step $a\bar{a}$, $\bar{a}a$, $b\bar{b}$ or $\bar{b}b$ otherwise the considered geometric figure is not a union of unit squares and thus the coded object could not be a polyomino.

For example, the boundary word of the mino is $ab\bar{a}\bar{b}$ and all cyclic permutations of letters $b\bar{a}\bar{b}a$, $\bar{a}\bar{b}ab$ and $\bar{b}ab\bar{a}$ leads to different boundary words depending where the starting point is taken. Nevertheless each cyclic permutation of letters define the same polyomino (Fig. 11).
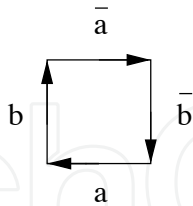

Figure 11. Coding of the boundary of the mino

Thus for a boundary word $w = w_1 w_2 \cdots w_n$ where all the w_i are letters that is $w_i \in \Sigma = \{a, b, \bar{a}, \bar{b}\}$ we define the conjugate of a boundary word w if $w = uv$ then a conjugate is defined by vu. We read on Fig. 11 the following boundary word of a mino $\bar{a}\bar{b}ab$ and we construct the 3 other possible boundary words (by changing the origin of the reading) by the notion of conjugate : we construct $b\bar{a}\bar{b}a$ by taking $u = \bar{a}\bar{b}a$ and $v = b$, we construct $ab\bar{a}\bar{b}$ by taking $u = \bar{a}\bar{b}$ and $v = ab$ and we construct $\bar{b}ab\bar{a}$ by taking $u = \bar{a}$ and $v = \bar{b}ab$.

This notion of boundary word is efficient because each polyomino can be characterized by it's boundary word.

For example the L-triomino could be defined directly by it's boundary word $b\bar{a}\bar{b}\bar{a}\bar{b}aab$ (Fig. 12). Remark that each conjugate of the word $b\bar{a}\bar{b}\bar{a}\bar{b}aab$ leads to the same L-triomino shape.
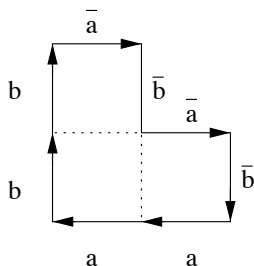

Figure 12. Coding of the boundary of the L-triomino

We know define a formal operation on words over the alphabet $\Sigma = \{a, b, \bar{a}, \bar{b}\}$. This operation will be crucial to define interfaces between tiles and for us abstract interfaces between chains.

We define the $\overline{u}$ operator on the word over the alphabet Σ by

if a word w of length n is written $w = w_1 w_2 \cdots w_n$ where all the w_i are letters that is $w_i \in \Sigma = \{a, b, \bar{a}, \bar{b}\}$

$(i)\overline{w} = \overline{w_n} \ \overline{w_{n-1}} \cdots \overline{w_1}$

$(ii)\overline{\bar{a}} = a$ and $\overline{\bar{b}} = b$.

The point (i) means that to use the bar operator on a word w, we bar each letter of the word w read in reverse order. The point (ii) means that 2 times the operator bar on a letter is equal to this letter.

In fact, if w is a part of a boundary word read clockwise then $\overline{w}$ is the same path read anti clockwise ! In Fig. 13 we see an example of a path clockwise associated with $w = b\bar{a}b\bar{a}b$ and the same path anti clockwise that is associated with $\overline{w} = \overline{b\bar{a}b\bar{a}b}$ by using the point (i) we reverse the word and take the bar of each letter and thus find $\overline{w} = \bar{\bar{b}}\bar{\bar{a}}\bar{b}\bar{\bar{a}}\bar{b}$ and by simplification according to the point (ii) we finally have $\overline{w} = baba\bar{b}$.
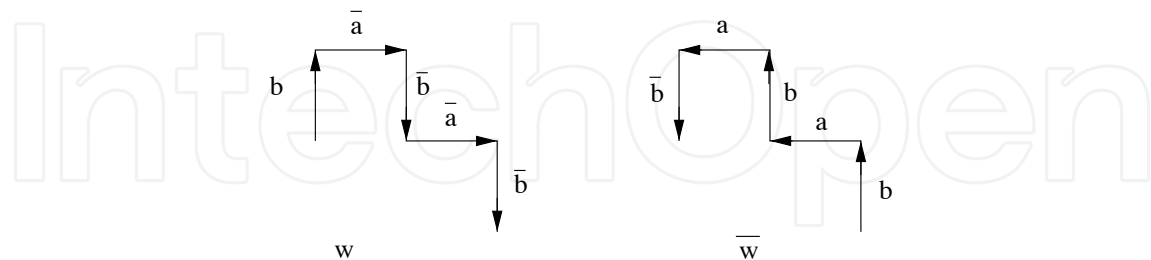

Figure 13. Coding of a finite path clockwise and anti clockwise

In a tiling of the plane each tile are surrounded by a certain number of adjacent copies of P. The spirit of the Beauquier-Nivat's Theorem [1] is that by investigating carefully a boundary word of P we could recover the possible surrounding of P.

Theorem 3.1 (Beauquier, Nivat). *A polyomino P tiles the plane by translation if and only if the boundary word $\mathbf{b}(P)$ is equal up to a cyclic permutation of the symbols to the factorization $X \cdot Y \cdot Z \cdot \overline{X} \cdot \overline{Y} \cdot \overline{Z}$ where one of the variables in the factorization may be empty.*

If the boundary word is equal to $X \cdot Y \cdot Z \cdot \overline{X} \cdot \overline{Y} \cdot \overline{Z}$ such a polyomino is called *pseudo hexagon*, if it is equal to $X \cdot Y \cdot \overline{X} \cdot \overline{Y}$ such a polyomino is called *pseudo square*.

Examples of factorizations and associated tilings of the plane.

A mino has a unique factorization on pseudo square, indeed the boundary word is $\mathbf{b}(P) = ab\bar{a}\bar{b}$ thus $X = a$ and $Y = b$ and $\overline{X} = \bar{a}$ and $\overline{Y} = \bar{b}$. In fact a mino tiles in a unique way and has the property that each tile is surrounded by 4 adjacent tiles (Fig. 14).
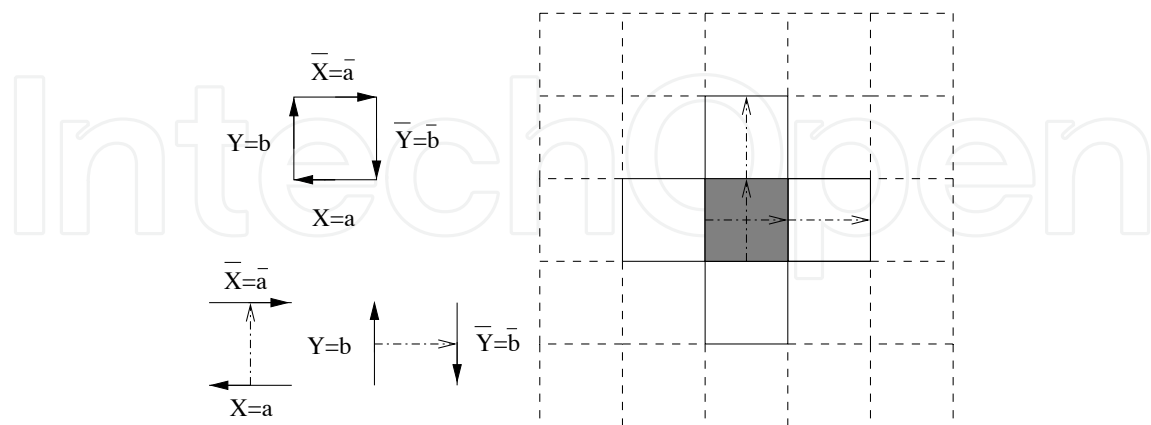

Figure 14. Tiling by a mino and the 4 adjacent tiles of the grey mino

A horizontal domino has exactly 2 factorizations $\mathbf{b}(P) = aab\bar{a}\bar{a}\bar{b}$ one in pseudo square by taking $X = aa$ and $Y = b$ and $\overline{X} = \bar{a}\bar{a}$ and $\overline{Y} = \bar{b}$ and given a tiling like a "non robust brickwall". In this case each tile is surrounded by 4 adjacent tiles (Fig. 15).
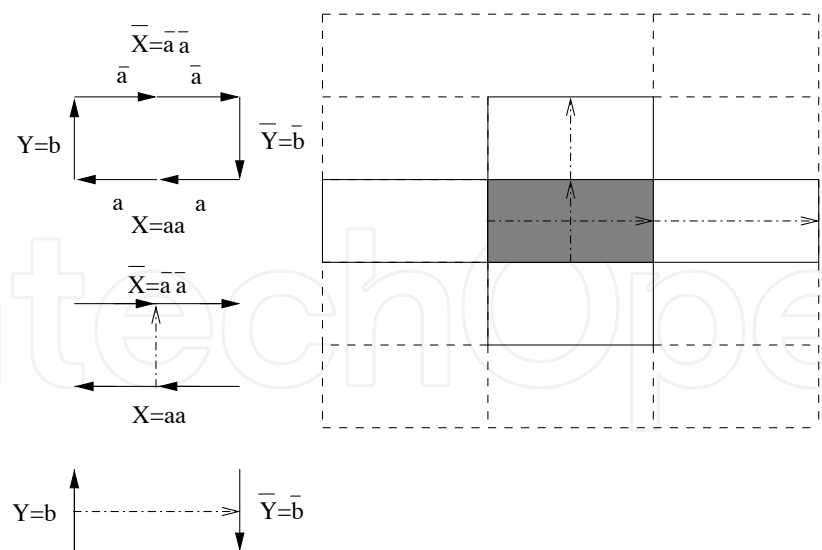
Figure 15. Tiling of the plane by a domino like a pseudo square and the 4 adjacent tiles of the grey domino

One factorization in pseudo hexagon by taking $X = a$, $Y = a$, $Z = b$ and $\overline{X} = \bar{a}$, $\overline{Y} = \bar{a}$, $\overline{Z} = \bar{b}$ which give a tiling like a "robust brickwall". In this case each tile is surrounded by 6 adjacent tiles (Fig. 16).
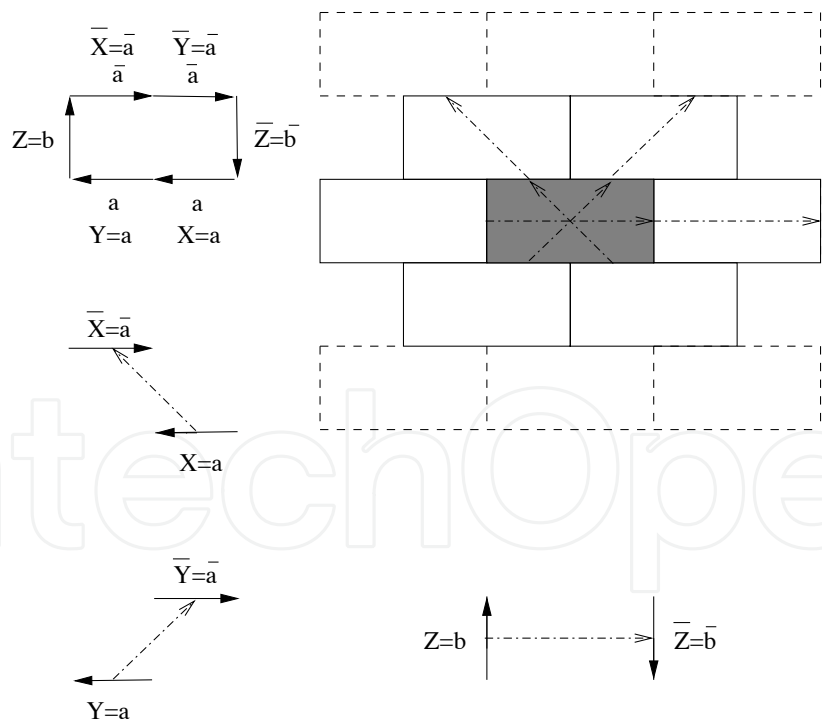

Figure 16. Tiling of the plane by a domino like a pseudo hexagon and the 6 adjacent tiles of the grey domino

Remark that the difference between the 2 tilings by a horizontal domino is the number of adjacent copies of polyominoes that surround the domino at the origin. Thus a domino tiles either like a pseudo square if the number of adjacent tiles of each tile is 4 or like a pseudo hexagon if the number of adjacent tiles of each tile is 6.

For the thin cross with 9 unit squares with boundary word equals to $a a b \bar{a} \bar{a} b b \bar{a} \bar{b} \bar{b} \bar{a} \bar{a} \bar{b} a a b \bar{b} b a b b$ it is impossible to find a factorization and this proves that the thin cross doesn't tile the plane anymore (the square with the symbol "?" cannot be covered) (Fig. 17).
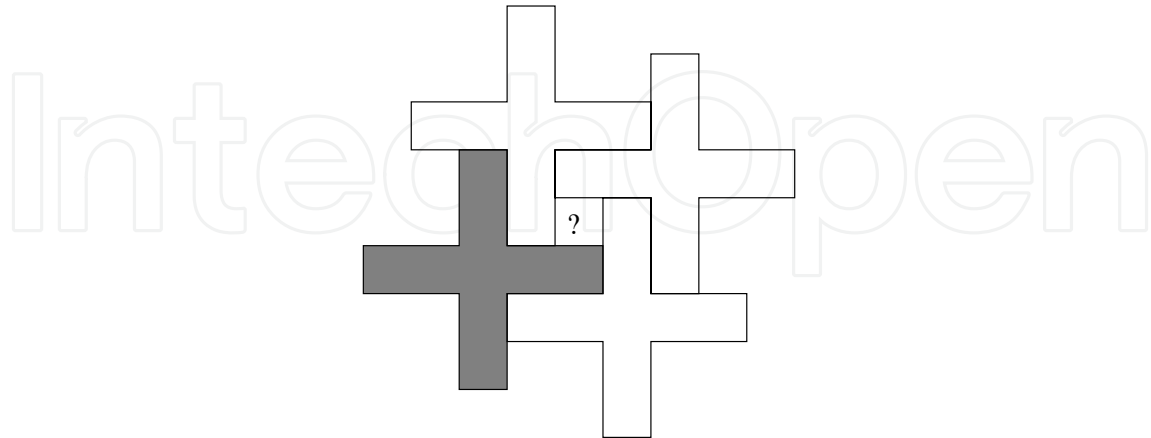

Figure 17. A thin cross that doesn't tile the plane

The triomino L with boundary word equals to $b \bar{a} \bar{b} \bar{a} \bar{b} a a b$ has only one factorization in pseudo hexagon, thus it tiles the plane in a unique way (Fig. 18).
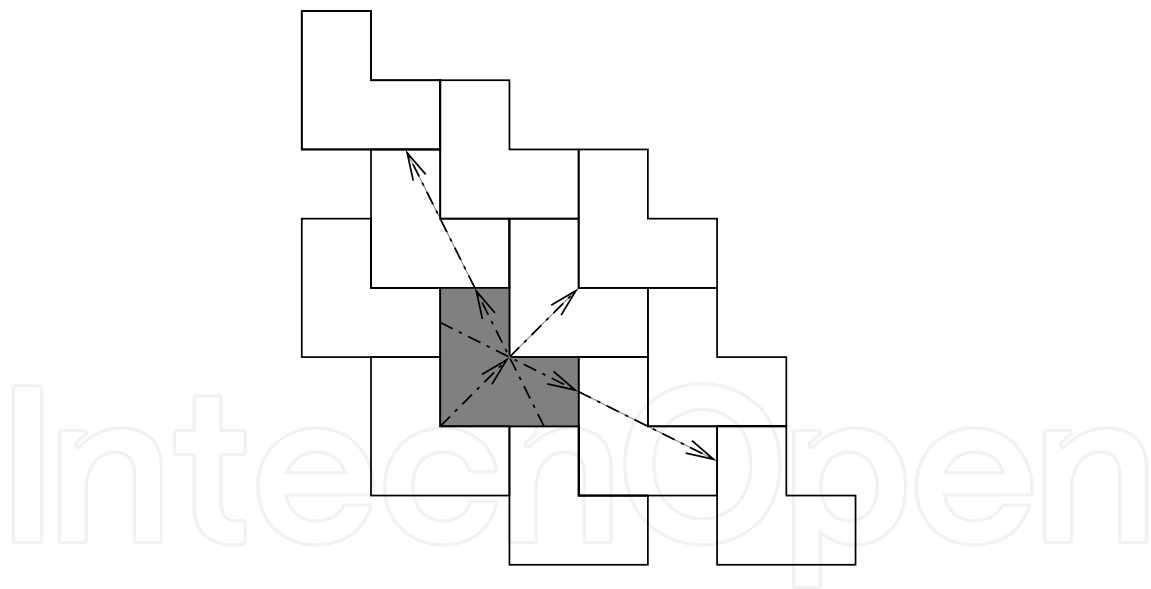

Figure 18. The *L*-triomino tiles the plane like a pseudo hexagon

While the little thin cross with 5 unit squares with boundary words $a b \bar{a} b \bar{a} \bar{b} \bar{a} \bar{b} a b a b$ has 2 factorizations in pseudo squares and thus 2 distinct tiling ways according to the 2 factorizations with $X = aba, Y = b\bar{a}b$ and with $X = bab, Y = \bar{a}b\bar{a}$ (Fig. 19).

To summarize, for each polymino we are able to decide if it tiles the plane by translation by considering the factorization of it's boundary word. Now, we investigate regular tilings of the plane.
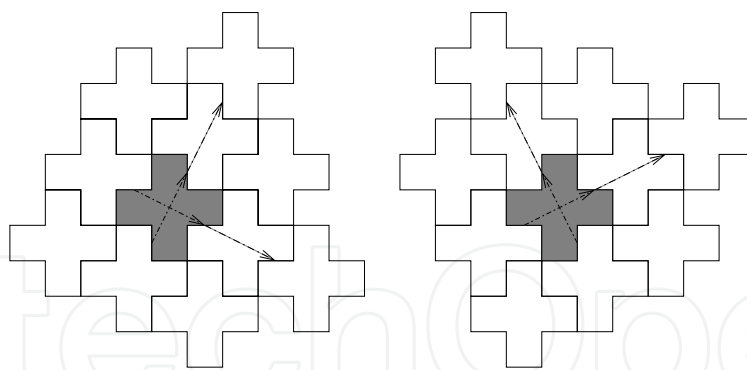
Figure 19. The 2 tilings like a pseudo square by a thin cross with 5 unit squares

4. Regular tilings by translation

The theorem of Beauquier-Nivat gives a correspondence between the way of tiling and the factorization that is the number of copies of the polyomino that surrounds a given polyomino. For the mino, we have 4 copies to cover the whole boundary (because a unit square is a pseudo square that tiles like a square). For the triomino L we have 6 copies to cover the whole boundary (because a triomino L is a pseudo hexagon that tiles like a hexagon). In fact we extend the local correspondences between the coding of part of the boundary word to a geometrical translations namely $\vec{v}_1$ translates X to $\overline{X}$ and $\vec{v}_2$ translates Y to $\overline{Y}$ (and possibly $\vec{v}_3$ translates Z to $\overline{Z}$). Remark that we have 2 or 3 translations according to the pseudo square or pseudo hexagon, respectively, and by translation to the whole tiling each polyomino has the same local surrounding.

It is interesting to introduce the notion of regular tiling. In a regular tiling the surrounding by adjacent tiles is the same for each polyomino. The mino and the triomino L tile only in a regular way by extending the local vectors to the whole tiling.

A *regular tiling* is a tiling by translation of a polyomino P such that each tile in the tiling has the same surrounding by translated copies of the tile P according to a given factorization of its boundary word. Each factorization leads to a regular tiling of the plane by translation by extending the local translation to the whole plane in the following way.

If P is a pseudo square, the factorization $\mathbf{b}(P) = X \cdot Y \cdot \overline{X} \cdot \overline{Y}$ defines 4 sides of the tile where the sides in correspondence are identified by the pairings $(X, \overline{X})$ and $(Y, \overline{Y})$. The translations $\vec{v}_1$, $\vec{v}_2$ corresponding to these pairings allow us to tile the whole plane in a regular way by using integral combinations of the translations $\vec{v}_1$ and $\vec{v}_2$ to P in order to generate the whole tiling (Fig. 14 or Fig. 15).

In the case of a pseudo hexagon the construction with 6 sides is similar. If P is a pseudo hexagon, the factorization $\mathbf{b}(P) = X \cdot Y \cdot Z \cdot \overline{X} \cdot \overline{Y} \cdot \overline{Z}$ defines 6 sides of the tile where the sides in correspondence are identified by the pairings $(X, \overline{X})$, $(Y, \overline{Y})$ and $(Z, \overline{Z})$. The translations $\vec{v}_1$, $\vec{v}_2$ and $\vec{v}_3$ corresponding to these pairings allow us to tile the whole plane in a regular way by using integral combination of the translations $\vec{v}_1$ and $\vec{v}_2$ to P in order to generate the whole tiling (Fig. 16 or Fig. 18) . Remark that the third vector of translation $\vec{v}_3$ is an integral combination of $\vec{v}_1$ and $\vec{v}_2$ ($\vec{v}_3 = \vec{v}_1 - \vec{v}_2$ in Fig. 16).

Observe that 2 distinct factorizations of the boundary word of P give 2 distinct regular tilings of the plane (Fig. 19 in the case of 4 adjacent tiles for each tile or Fig. 20 in the case of 6

adjacent tiles for each tile; be careful that while a regular tiling is always given by integral combinations of 2 vectors $\vec{v}_1$ and $\vec{v}_2$, the boundary of each tile in the pseudo hexagon case use 6 sides in correspondence 2-by-2 with the translations $\vec{v}_1$, $\vec{v}_2$ and $\vec{v}_3$). Are you able to recover the 6 adjacent polyominoes of the grey polymino of Fig. 20 ? Hint: in Fig. 20 one adjacency is only by a single vertical step (for the left regular tiling) or horizontal (for the right regular tiling) ...
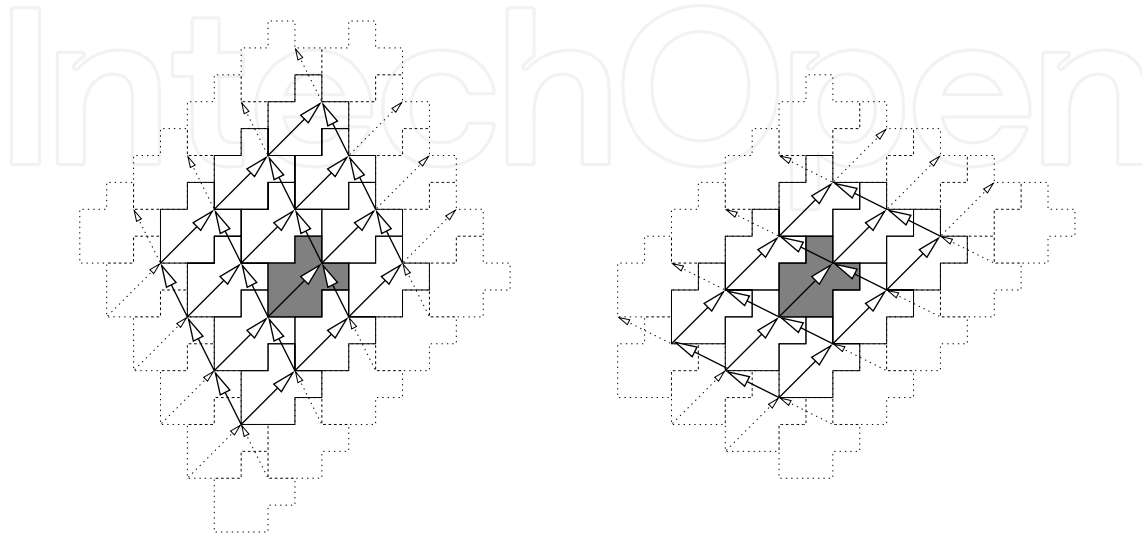

Figure 20. Two regular tilings of the plane by the same polyomino

5. From tilings of the plane to tilings of a fiber

5.1. Regular tiling case

From now on, we are dealing with the form of the oligomerization of proteins either like a cylinder or like a fiber. For us a cylinder has finite height (Fig. 1A) and a fiber is a possibly non finite height object (Fig. 25).

In our model we would like to make the construction of a fiber (that is a non finite height cylinder) by transformation on regular tilings. As the tiling is regular, the whole tiling is invariant by translation of the 2 non null and non collinear vectors $\vec{v}_1$ and $\vec{v}_2$ defined at the previous paragraph. $\vec{v}_1$ and $\vec{v}_2$ are the vectors of translations that respectively send X to $\overline{X}$ and send Y to $\overline{Y}$. In mathematics the parallelogram constructed by $\vec{v}_1$ and $\vec{v}_2$ at a given integer point is called the fundamental domain that is the minimal part of the tiling used to construct the whole tiling by integral combinations of $\vec{v}_1$ and $\vec{v}_2$.

Let $\vec{e}_1$ be a horizontal unit vector. We choose a direction parallel to $\vec{e}_1$ namely $m.\vec{v}_1 + n\vec{v}_2 = k.\vec{e}_1$ with m and n given integers. Then we construct the little circle (that is by usual definition the horizontal circle of the cylinder) whose perimeter is equal to k by superposing the tiles of the original tiling and the tiles translated by $k.\vec{e}_1$. Indeed as the tiling is invariant by translation of integral combination of $\vec{v}_1$ and $\vec{v}_2$ we are able recover the same shape by using the translation $m.\vec{v}_1 + n\vec{v}_2$ (which is by construction equal to $k.\vec{e}_1$). Fig. 21 shows an example of a cylinder constructed with a regular tiling by a mino using the identification of the two bold vertical borders for the translation $8\,\vec{v}_1$ (here for a mino $\vec{v}_1=\vec{e}_1$). In the associated cylinder

the two vertical borders are collapsed in a single border and this transformation is general as soon as we identify in the tiling two infinite borders in correspondence by a translation of vector $m.\vec{v}_1 + n\vec{v}_2$.
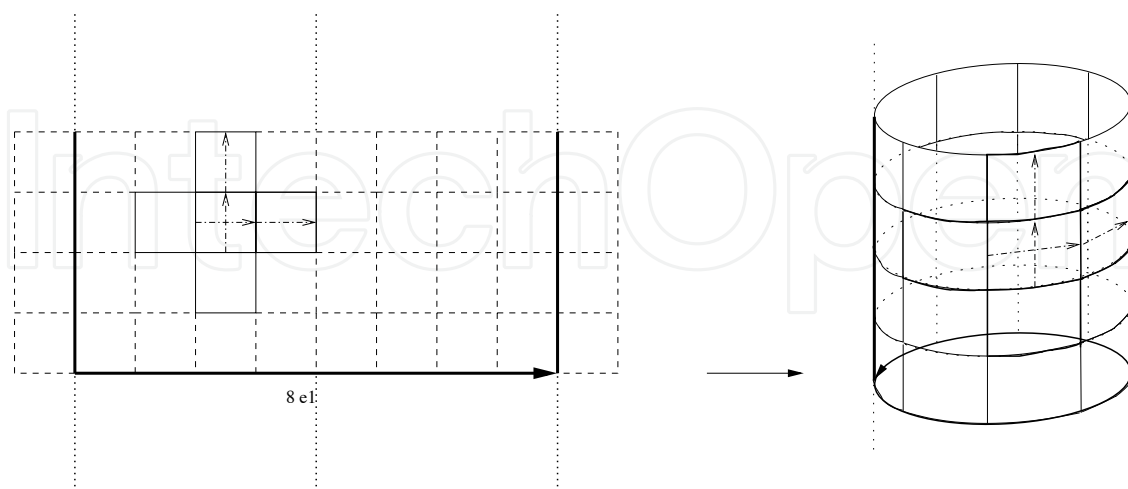

Figure 21. From tiling to cylinder by using the translation of 8 times the vector $\vec{e}_1$.

In the next example (Fig. 22), the vectors $\vec{v}_1$ and $\vec{v}_2$ send respectively $X = b\bar{a}b$ to $\overline{X} = \bar{b}a\bar{b}$ and $Y = aba$ to $\overline{Y} = \bar{a}\bar{b}\bar{a}$. In order to find a horizontal direction we take 2 times the vector $\vec{v}_1$ and 1 time the vector $\vec{v}_2$. Remark that the distance between the point O and the point O translated by $2\vec{v}_1 + \vec{v}_2$ is exactly 5. If we want a little circle with perimeter 10 we consider the translation $2 * (2\vec{v}_1 + \vec{v}_2)$ that is 4 times $\vec{v}_1$ and 2 times $\vec{v}_1$. Now we make a fiber by rolling up the plane by identification the 2 sides in bold (this is exactly the border of the tiling given by a staircase in correspondence by the translation with vector $4\vec{v}_1 + 2\vec{v}_2$) (Fig. 22). In order to have a more general construction and in particular to construct a twist in the fiber, we could use a rational coordinate vector $\vec{r}_1$ instead of $\vec{e}_1$ and find a direction parallel to $\vec{r}_1$ given by the equation $m\vec{v}_1 + n\vec{v}_2 = k\vec{r}_1$.

Conversely, if a polyomino tiles a fiber by translation we recover the whole tiling by finding the little circle and the invariance of the fiber by translation by $k.\vec{e}_1$ and considering in $\mathbb{R}^2$ the strip at the origin and adding all the strips on $\mathbb{R}^2$ by translation $\ell.k.\vec{e}_1$ with $\ell \in \mathbb{Z}$.

To summarize, in order to construct a model of fiber using a regular tiling by a single polyomino, the polyomino must tile the plane in a regular way and thus must have at least a factorization as a pseudo square or as a pseudo hexagon. In the fiber, if the tiling is regular then the number of adjacent copies that surround the border is either 4 or 6. This implies that the number of distinct interfaces is 2 or 3.

Of course the model is very flat and in real fibers the molecules are in a 3 dimensional space nevertheless this model allows us to make hypothesis about the number of interface sites and we try to find either 2 or 3 interface sites in the fiber.

We have explained that to build a fiber with a non finite height cylinder shape, it is necessary to have 2 vectors, namely 2 directions of polymerization growth. We have also seen that each tile of fiber will have 4 or 6 adjacent chains formed via 2 or 3 interfaces, respectively. There are examples of such fibers tiled with a single protein: the famous tobacco mosaic virus which was the first virus to be discovered has 4 adjacent chains to each chain (see Fig. 23 for
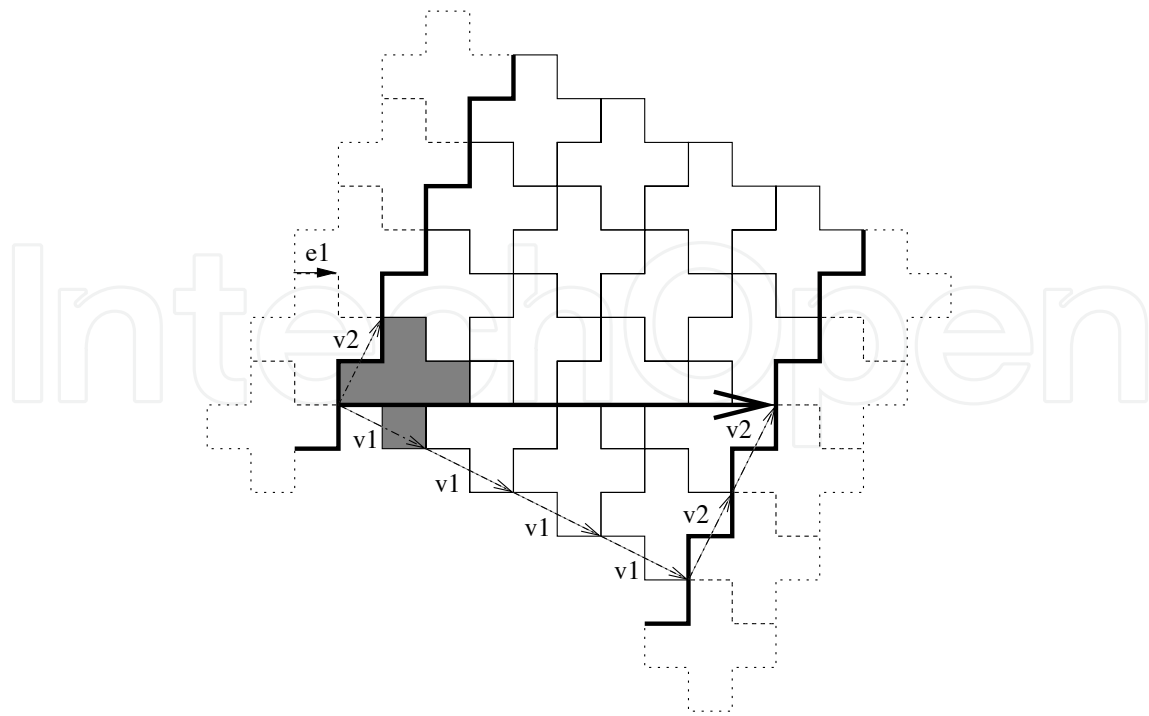
Figure 22. Two boundaries in correspondence by the translation $4\vec{v}_1 + 2\vec{v}_2$)

the abstract view and Fig. 24 for a part of a real fiber) and the polymerization in fiber with name 3J1R has 6 adjacent chains to each chain (see Fig. 25 for the abstract view and Fig.26 for a part of real fiber).

5.2. Tiling fibers by n-mers

This chapter is an investigation of the combinatorial possibilities on the construction of the fiber. Either a fiber is composed by a regular tiling by a single chain (Fig. 23 for the abstract view and Fig. 24 for a part of a real fiber with pseudo square tiling and Fig. 25 for the abstract view and Fig.26 for a part of real fiber with pseudo hexagon tiling) or the regular tiling of the fiber is composed by a n-mer (in mathematics we called this object a meta tile). Thus globally the fiber is a tiling by a meta-tile and this meta-tile could be a single chain or a n-mer.

In real life we find fibers tile either by a single chain or by a n-mer. In Fig. 27 we see a real fiber with name 3J2U constructed with a tetramer of three chains namely A, B and 2 times the chain C. The tetramer is used to tile the fiber of pseudo hexagon type like in Fig. 25 by substituting each pseudo hexagon by the tetramer $\begin{smallmatrix} A & B \\ C & C \end{smallmatrix}$. You will notice in the next section about p53, the final construction of the fiber uses tiling of dimers (see Fig. 33D).

Another example is the construction using oligonucleotides of DNA inspired by the seminal work of Winfree [37]. These technics lead to nano tubes composed by dimers surrounded by either 4 adjacent dimers [23] or 6 adjacent dimers [39].

Conway has a criterium for tiling the plane in the case of a tile and a rotation of the tile by 180 degrees. In his article, he forms a meta-tile using the tile T and it's rotation $\text{Rot}_{180}(T)$ and this meta-tile is able to tile the plane by translation. Guy Cousineau wrote an article to
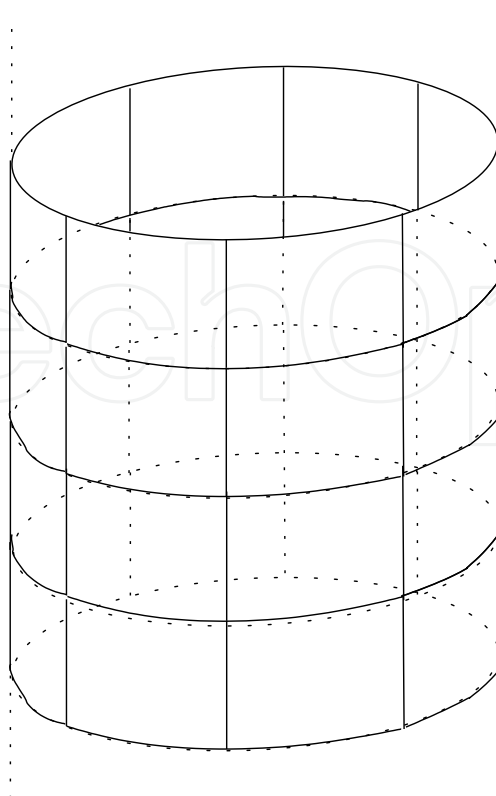
Figure 23. Fiber with a pseudo square shape. Each tile is surrounded by 4 tiles.
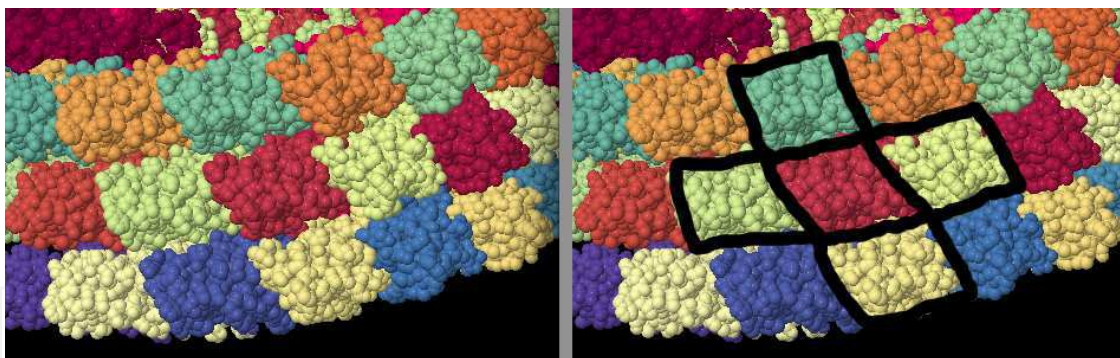

Figure 24. Tobacco Mosaic Virus with 2TMV PDB code: an example of tiling of a fiber with 4 adjacent chains.

explain the combinatorics of tilings with axial symmetry and translation (see the chapter of Cousineau in this book). In real life, fibers could be constructed for example with dimers. In general the dimer in the fiber is either invariant by a rotation of 180 degrees or invariant by an axial symmetry and then the dimer is used to tile by translation a fiber (see Fig. 28). Thus our model allows us to first make an interface for forming the dimer. And eventually to make a fiber by translation of the dimer according to the tiling constraints that is by having exactly 2 or 3 interfaces for the tiling of the fiber by the dimer. To recap we have constructed either 3 (one for the dimer and 2 for a tiling like a pseudo square) or 4 interfaces (one for the dimer and 3 for a tiling like a pseudo hexagon).
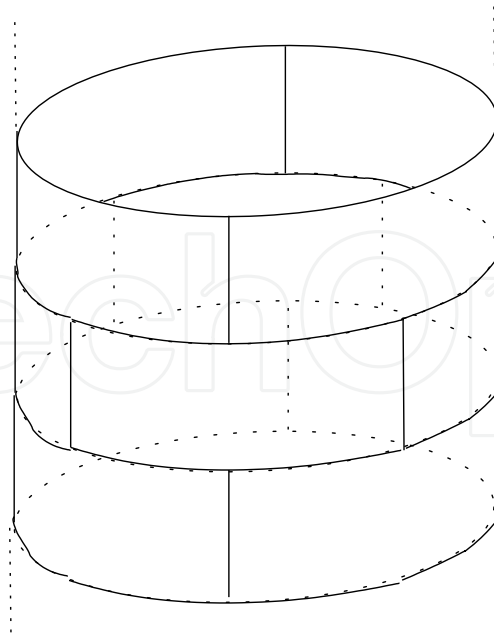
Figure 25. Fiber with a pseudo hexagon shape. Each tile is surrounded by 6 tiles. Remark that pseudo hexagon shapes appear in particular when there is a tilt on the fiber.
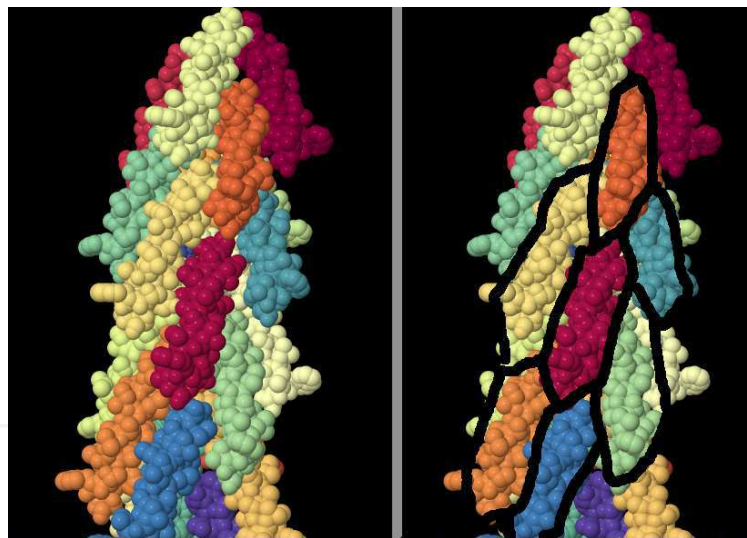

Figure 26. Fiber with 3J1R PDB code: an example of tiling of a fiber with 6 adjacent chains.

For higher stoichiometry, we construct a n-mer invariant by rotation of $360/n$ degrees and we copy this meta-tile in order to tile the whole fiber (see Fig. 29 for an abstract view of the replacement by a tetramer).

According to the previous tiling constraints, as the number of sites is 2 or 3 it is more easy to make a fiber with a monomer, dimer, trimer, tetramer and hexamer because we combine the shape of the n-mers with the form of the interfaces in order to build the whole fiber. We think that the better values are 1, 2, 3, 4, 6 because these values are also in accordance with the crystallographic constraints (the laws of crystallography [31] allow only periodical tilings with rotations of order 1,2,3,4 and 6, that is by rotations of $360, 180, 120, 90$ or 60
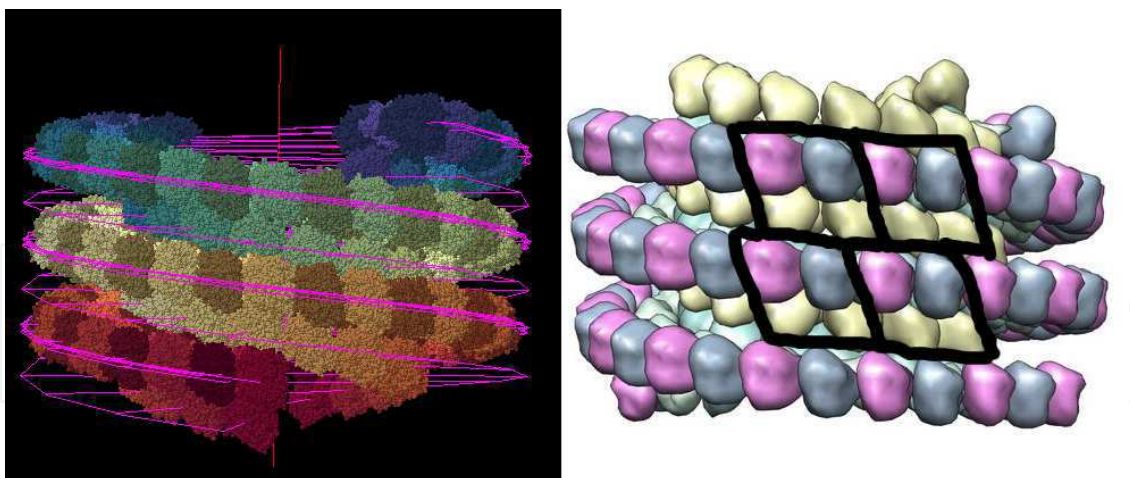
Figure 27. Fiber with 3J2U PBD code containing a tetramer inside each pseudo hexagon
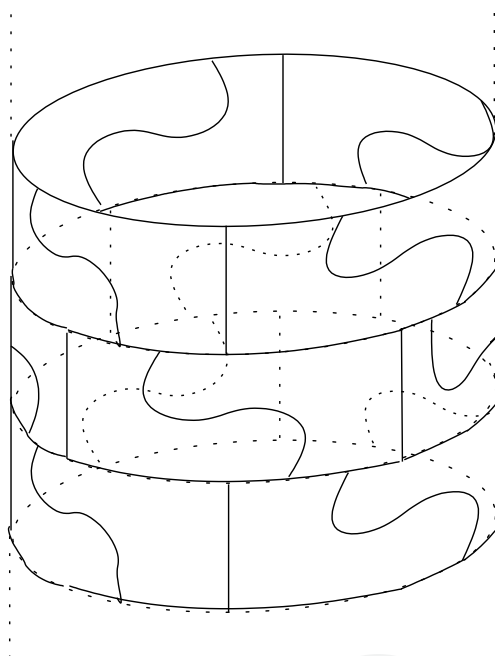

Figure 28. Fiber with a dimer inside each pseudo hexagon

degrees). Of course accordingly a transition from pentamer or heptamer ($n = 5$ or 7) to fiber would be expected to be more difficult at least with the mechanism described in this chapter. In this direction quasicrystals come from aperiodical tilings of the whole plane and non periodical structures could appear in viruses [35], nevertheless non periodical ways to form a fiber by translation of a single tile is described in the next section. Indeed, to form Penrose like tilings we must have two tiles with aperiodic arrangements [5, 31] and it is still an open problem to find an aperiodic tiling of the whole plane with a single tile [15] (we expect by the theorem of Beauquier-Nivat that the boundary of such tile (if it exists) must be fractal...). In our fiber model the rules seem to be restrictive because such symmetry fits directly without deformation into a square or hexagonal tile. Of course in real life, the n-mers could be symmetrical ([17, 22, 24]) but also non-symmetrical ([4, 32]). We think that for tiling constraints on the border of each n-mers the less expansive solution in order to construct a
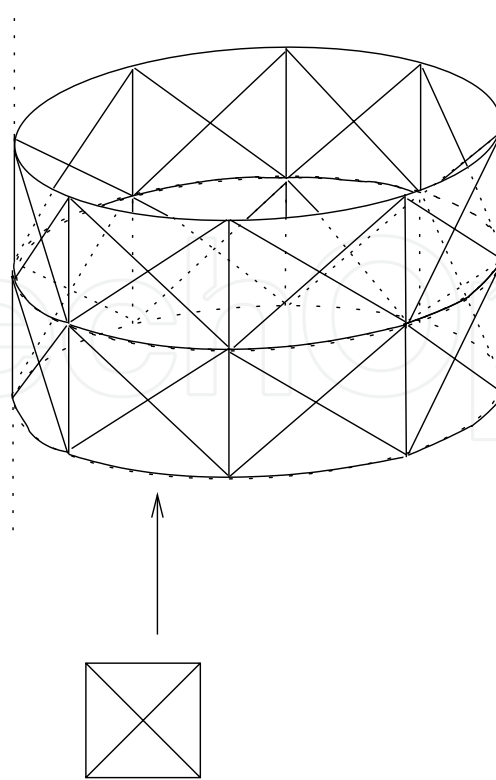
Figure 29. Replacement of each pseudo square by a tetramer.

fiber is given by symmetrical n-mers. On the other hand, dimers of pentamer or heptamers are able to fit with some deformations a hexagonal tile ie not all monomers are identical (Fig. 31). Such a dimer of pentamer has been observed in nature e.g. synthetic tachylectin (PDB 3KIF, Fig. 32) (see [38]).

Likewise the pore forming toxin aerolysin can form a dimer of heptamer after a single amino acid mutation (see [33]). It remains to be established whether the dimeric versions of the pentamer and heptamer are more prompt to form fibers than their single oligomeric counterpart. Of course the combinatoric is more and more complicated for $n > 7$ and to construct the fiber the position of the interfaces on the pseudo square or on the pseudo hexagon is split in different parts for $n > 7$ and this construction is very constrained and maybe this phenomenon is difficult to see in real life. Nevertheless such fibers could be constructed in synthetic biology.

We give some examples of replacements of a pseudo square by a dimer, by a tetramer and by an octamer and of a pseudo hexagon by a dimer, by a trimer and by a hexamer (see Fig. 30).

5.3. From fold plasticity to fibers: the P53 case

Notice that the main difference between tiling a finite height cylinder and tiling a fiber (an infinite height cylinder) is the number of directions of the polymerization growth, one in the former case and two in the latter case. Thus a transition from a cylinder to a fiber implies a transition from a single interface to 2 (4 adjacent chains) or 3 interfaces (6 adjacent chains). For this to occur one simple possibility is to start from an oligomer which has 2 regions of interfaces and loosen the constraints on one so it opens to bind in another direction. Common
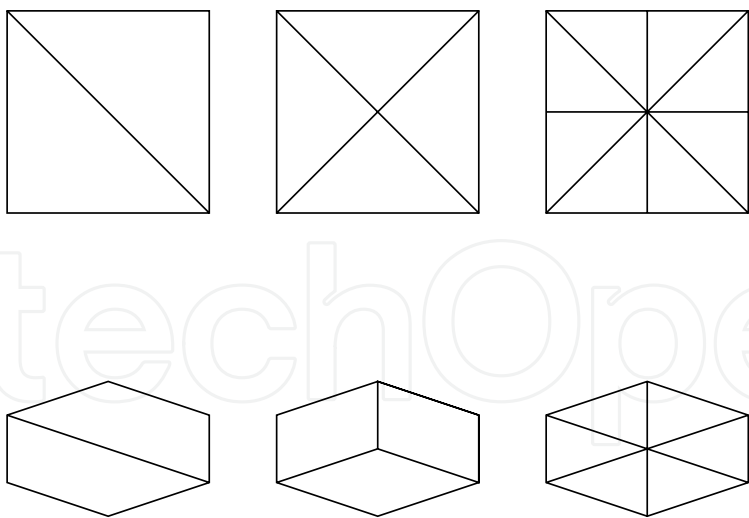
Figure 30. Replacement of a pseudo square and of a pseudo hexagon.
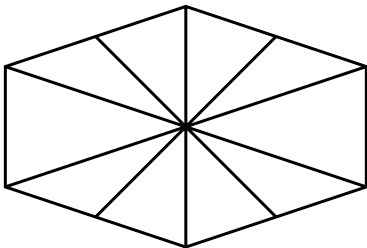

Figure 31. Replacement of pseudo square by 2 non regular pentamers.

Figure 32. Double asymmetrical pentamer.

biological examples of such transition are domain swapping ([9, 25]) where the presence of a flexible linker frees one interface for fiber formation.

Another possibility is to start from a dimer with 2 regions of interfaces and again loosen one of the region but this time via a mutation. If the modified residue controlled the interactions between the 2 regions, its modification may loosen one region opening it to form a second interface. Since the initial molecule is a dimer, the mutation will free 2 new interfaces enabling the growth in 2 directions. The formation of the fiber will depend on the symmetry of the dimer. To illustrate this possibility, let's consider the p53 tetramer (see Fig. 33). There are several familial point mutations such as G334V or R337 that are responsible for the transition of the p53 into fibers or into a non-native oligomeric state, leading to impairment of the protein function and cancer development [27]. p53 tetramer has a D_2 symmetry and is a dimer of a dimer. Each monomer is made of a β-strand, a small helix and a long α-helix (Fig. 33B). Contacts exist between the residue R337 of the small helix and the residues E349 and D352 of the long helix of the adjacent chain within a dimer of p53 (Fig. 33A). There are contacts between the residues L350 and K351 of one monomer of a dimer and the same residues on another monomer of another dimer (Fig. 33A). The mutation of R337 might inhibit the formation of the small helix and replace it by a more flexible linker which would be too mobile to allow the contacts with the residues E349 and D352 and might also subsequently loosen the contacts between L350 and K351 (Fig. 33B and C). As a consequence the relative position of the β-strand and the long α-helix would be altered allowing the formation of 2 new interfaces (Fig. 33D).

6. Non periodical fiber case and tiling of the whole space case

6.1. From 1-periodical tiling to fibers

In fact, all the preceding constructions are based on regular tilings of the plane. We are able to relax this constraint and to investigate non regular tilings (Fig. 34). Non regular tilings of the plane are constructed by perturbation of regular tilings. We push some strips in the direction $\vec{v}_1$ in order to break the periodicity in direction $\vec{v}_2$. In the seminal article of Beauquier-Nivat [1] an important proposition is proved that a tiling (regular or not) by translation of a polyomino is always 1-periodic that is invariant by a translation by a non null vector. This proposition is crucial for us because it allows to take a non regular tiling by a polyomino P and to map it on a fiber.

We take a given tiling T by translation of a given polyomino P and as the tiling T is 1-periodic it is invariant by vector $\vec{v}_1$. Thus we have the property that the translation by $\vec{v}_1$ of the tiling T noted $\text{Trans}_{\vec{v}_1}(T)$ is equal to the tiling T (here to be more formal and to define the equality between tilings we must introduce equivalent classes of tilings up to translation operator but it is too formal for this chapter written for biologists). By composition of the translations, we have that the translation of k times the vector $\vec{v}_1$ of the tiling T is also equal to the tiling T. That is $\text{Trans}_{k.\vec{v}_1}(T) = T$. Thus globally the tiling T is invariant by the translations $k.\vec{v}_1$ for $k \in \mathbb{N}$.

This global property of invariance of the tiling T implies a strong property on the boundary word of P. In fact in the original article of Beauquier-Nivat the following proposition: if the tiling T is 1-periodic then the boundary word is of the form $XW\overline{X}V$ with $W = U^r$ and $V = \overline{U}^r$. Thus locally in the boundary word we are able to read the periodicity property.
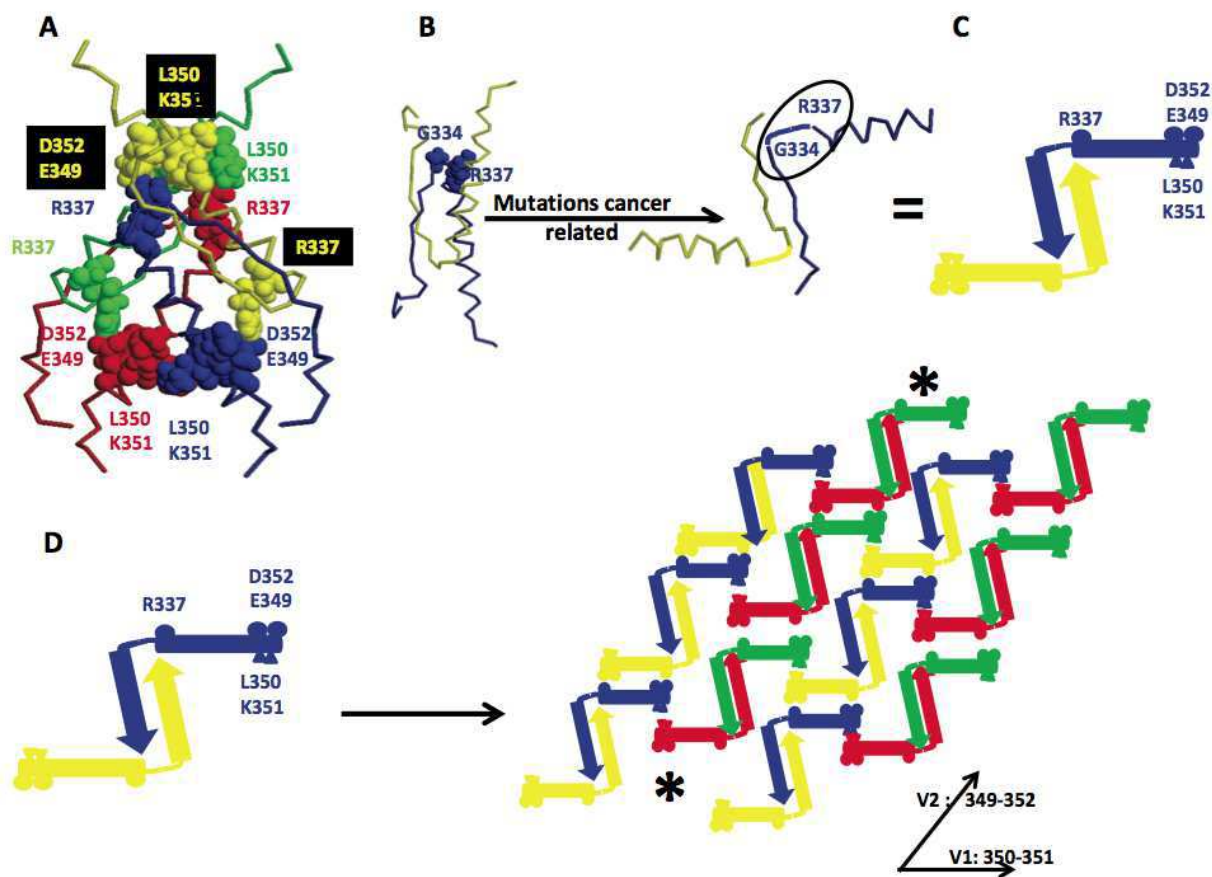
Figure 33. **Transition from oligomer to fiber, the example of the p53 case. A. The p53 tetrameric domain is made of 2 dimers.** Each monomer is made of a β-strand followed by a small helix ended by a long α-helix parallel to the β-strand (1SAK, PDB code). The backbone of each monomer is indicated by a different color. The spacefill amino acids are the residues in contact with R337, which is a residue sensitive to mutation related to some cancer development. **B. Backbone representation of the p53 dimer.** The model proposes that upon mutation of R337, connections between the 2 monomers within a dimer are loosen, enabling a free movement of the long α-helix relative to the β-strand. C. Schematic of the open-p53 dimer. D. As the structural change takes place in the four monomers, it offers enough new interfaces for growing in 2 directions $\vec{V}_1$ and $\vec{V}_2$.

For example for a bar of 5 unit squares with boundary word $abbbbb\bar{a}\bar{b}\bar{b}\bar{b}\bar{b}\bar{b}$, we have many factorizations one in pseudo square by taking $X = a$ and $Y = bbbbb$ and $\overline{X} = \bar{a}$ and $\overline{Y} = \bar{b}\bar{b}\bar{b}\bar{b}\bar{b}$ and 4 four factorisations in pseudo hexagon by taking $X = a$ and $Y = b$ and $Z = bbbb$ and $\overline{X} = \bar{a}$ and $\overline{Y} = \bar{b}$ and $\overline{Z} = \bar{b}\bar{b}\bar{b}\bar{b}$ or $X = a$ and $Y = bb$ and $Z = bbb$ and $\overline{X} = \bar{a}$ and $\overline{Y} = \bar{b}\bar{b}$ and $\overline{Z} = \bar{b}\bar{b}\bar{b}$ or ... or $X = a$ and $Y = bbbb$ and $Z = b$ and $\overline{X} = \bar{a}$ and $\overline{Y} = \bar{b}\bar{b}\bar{b}\bar{b}$ and $\overline{Z} = \bar{b}$. In this example the periodic part on the boundary word is $U^5 = bbbbb$ with $U = b$ and $\overline{U}^5 = \bar{b}\bar{b}\bar{b}\bar{b}\bar{b}$. Remark that in this case $U^5 = bbbbb$ appears in the factorization in pseudo square.

Another example without factorization in pseudo square is a polyomino constructed by union of 3 triomino L and forming a polyomino with 9 unit squares with boundary word $\bar{b}aababab\bar{a}b\bar{a}\bar{b}\bar{a}\bar{b}\bar{a}\bar{b}$ here the factorizations are

$X = \bar{b}a$ $Y = a$ $Z = babab$ $\overline{X} = \bar{a}b$ $\overline{Y} = \bar{a}$ $\overline{Z} = \bar{b}\bar{a}\bar{b}\bar{a}\bar{b}$ or $X = \bar{b}a$ $Y = aba$ $Z = bab$ $\overline{X} = \bar{a}b$ $\overline{Y} = \bar{a}\bar{b}\bar{a}$ $\overline{Z} = \bar{b}\bar{a}\bar{b}$ or $X = \bar{b}a$ $Y = ababa$ $Z = b$ $\overline{X} = \bar{a}b$ $\overline{Y} = \bar{a}\bar{b}\bar{a}\bar{b}\bar{a}$ $\overline{Z} = \bar{b}$. In this case $U^3 = ababab$ with $r = 3$ and $U = ab$ and $\overline{U}^3 = \bar{b}\bar{a}\bar{b}\bar{a}\bar{b}\bar{a}$ with $r = 3$ and $\overline{U} = \bar{b}\bar{a}$. Remark that in this case U^3 does not appear in the boundary word factorization and is splited in 2 parts, one is Y and
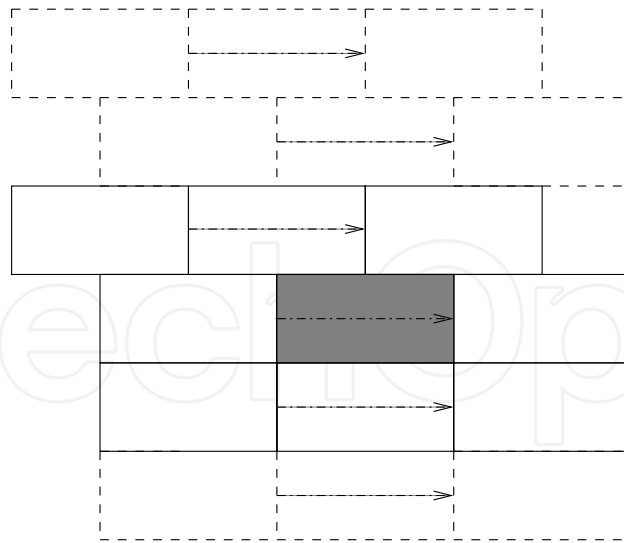
Figure 34. Non regular tiling with dominoes. The grey domino is surrounded by 5 dominoes thus this tiling is certainly not regular. Remark that the horizontal strips are invariant by the horizontal vector $\vec{v}_1$ and also by the vector $3\vec{v}_1$. Thus we are able to map the left border to the right border in order to form a non finite height cylinder.

the second is Z because $W = U^3 = YZ$. Remark in the picture the periodic part in a staircase shape (Fig. 35).
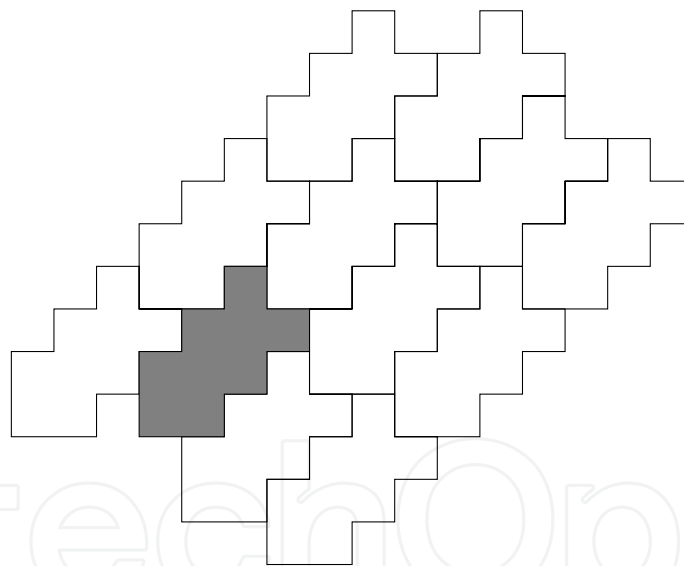

Figure 35. Non regular tiling and stair case shape.

This condition on the border is a necessary condition to find a possible periodicity. In particular, if we want to make the tiling 1-periodic we must push the strip along this direction of periodicity.

In order to construct a fiber we take the tiling and map it on a fiber by superposing tiles according to the direction of periodicity given by $\vec{v}_1$. Now we choose a non null value for k, we are able to construct a fiber because the whole tiling is invariant by the translation $k\vec{v}_1$ and we superpose the tiles of the original tiling and the tiles translated by $k\vec{v}_1$. Thus we make a fiber that contains exactly k polyominoes along the direction $\vec{v}_1$. An important implication

of this construction is the possibility of shifting the strips using the stair case shape. This means that the fiber has one degree of liberty and can tilt along the periodic direction.

6.2. From fibers to tilings of the space

To end this section we give some hints about a possible transition from fiber to tiling of the whole 3 dimensional space. In fact the protein chains are in a 3 dimensional space and we could investigate regular tiling of a 3 dimensional space by a translation of a single polycube (generalization in 3D of the polyomino) that is a union of unit cubes face to face. Such kind of regular tilings leads to tile the whole space by using 3 vectors of translation and in [14] Gambini and Vuillon show that the surrounding of a tile could have n adjacent tiles with a fixed integer $n \geq 6$. For tiling the plane or fibers the number of interfaces is finite and equals to 2 or 3 and in contrast for tiling the space by a polycube the number of interfaces could be greater than each integer n with $n \geq 3$. This means that the number of interfaces could not be finite a priori (see [14]). One interesting question is the following, could we observe in real life a transition by fold plasticity from a fiber to a tiling of the whole 3 dimensional space ?

7. Conclusion

In this chapter, we focus on mathematical aspects of fibers. The main goal consists on the explanation of basic rules in order to construct cylinders or fibers based on regular tilings by translation of a single chain or of a juxtaposition of chains forming a n-mer. We notice that the interfaces must be 2 or 3 according to the tiling on pseudo squares or pseudo hexagons. This is the basic construction and leads to a fiber with a pseudo square tile or with a pseudo hexagon tile. Now, in order to add more combinatorial complexity, we are able to replace each tile on the fiber by a n-mer constructed by adding at least another interface. This result inherits the strong combinatorial properties of tilings by polyominoes explored by Beauquier and Nivat [1, 13] and we add the power of combinatorial construction of the n-mers. We could now use this construction to explore the structure of real fibers or to construct synthetic fibers. The steps of investigation will be the following: first we look globally at the fiber by searching the smallest object that tiles the fiber (Fig. 23 for the abstract view with pseudo square tiling and Fig. 24 for a part of a real fiber and Fig. 25 for the abstract view with pseudo hexagon tiling and Fig.26 for a part of real fiber). If this object (called meta-tile) is a single chain then we stop the investigation because the structure is found. Otherwise the meta-tile that tiles the fiber is composed by a n-mer and we investigate carefully the structure of this n-mer (in Fig. 25 the tiling meta-tile is a 4-mer with form $\begin{smallmatrix} A & B \\ C & C \end{smallmatrix}$ and in the p53 fiber, the object is a 2-mer (see Fig. 33D). Thus each fiber is composed if we zoom out by a tiling by translation by a meta-tile which is a pseudo square or is a pseudo hexagon and if we zoom in the meta-tile is a n-mer. Of course if $n = 1$ then the tiling is by a single chain and if $n \geq 2$ the tiling of the fiber is done by a meta-tile which is a n-mer. Remark that for $n = 1$ as we tile by a single shape the number of interfaces is 2 for the pseudo square case or 3 for the pseudo hexagon case. If $n \geq 2$ then we must add at least 1 interface to form the n-mer and thus globally the number of interfaces is at least 3 for the pseudo square case or 4 for the pseudo hexagon case. Our model covers all cases because by zooming in the meta-tile inherits the intrinsic combinatorial complexity of the n-mer construction and by zooming

out we recover the 2 ways of tilings either by a pseudo square or a pseudo hexagon. Now we have a complete theory of fiber construction in biology and new robust bio-mathematical tools in order to reinvestigate our favorite fibers.

A future exploration can select from the entire PDB, the structures with the global symmetry most appropriate for fiber formation. This set can be screened further for isolating oligomers with only 2 interfaces or only 3 interfaces. These oligomers contain the necessary elements for fiber formation. We can then sort the dataset into two categories, cases known to form pathological fibers and the others. Comparing the characteristics of the interfaces of the cases whose fate is to become pathological fibers and of the "non pathological" cases would help distinguishing the parameters providing the plasticity needed for the transition to fiber from the parameters providing resistance to fiber formation.

Acknowledgements

Author details

C. Lesieur[1] and L. Vuillon[2*]

*Address all corespondence to: Laurent.Vuillon@univ-savoie.fr
1 Université Joseph Fourier, AGIM, Grenoble, France
2 Laboratoire de mathématiques, Université de Savoie, France

References

[1] Beauquier D. and Nivat M., On translating one polyomino to tile the plane, *Disc. Comput. Geom.*, 6 (1991) 575-592.

[2] Bellotti V., Chiti F. (2008) Amyloidogenesis in its biological environment: challenging a fundamental issue in protein misfolding diseases. Current opinion in structural biology 18: 771-779.

[3] Bernstein, F. C., Koetzle, T. F., Williams, G. J., Meyer, E. F., Jr., Brice, M. D., Rodgers, J. R., Kennard, O., Shimanouchi, T., and Tasumi, M. (1977) The Protein Data Bank. A computer-based archival file for macromolecular structures. Eur J Biochem 80, 319-324

[4] Brown, Jerry H. (2006) Breaking symmetry in protein dimers: Designs and functions. Protein Science,15:1,1–13.

[5] de Bruijn, N. G. (1981) Algebraic theory of Penrose's nonperiodic tilings of the plane. I, II. Nederl. Akad. Wetensch. Indag. Math., 1:43, 39–66.

[6] Cheng P.-N., Pham J.D. and Nowick J.S. (2013). The Supramolecular Chemistry of β-Sheets. Journal of the American Chemical Society.

[7] Chiang P.K., Lam M.A. and Luo Y. (September 2008). "The many faces of amyloid beta in Alzheimer's disease". Current molecular medicine 8 (6): 580–4. doi:10.2174/156652408785747951. PMID 18781964.

[8] Claverie, P. and Hofnung, M. and Monod, J. (1968) Sur certaines implications de l'hypothese d'équivalence stricte entre les protomeres des protéines oligomériques. CR Séanc. Acad. Sci 266, 1616–1618.

[9] Eisenberg D. and Jucker M. (2012). The Amyloid State of Proteins in Human Diseases. Cell 148: 1188-1203.

[10] Ferreira S.T., Vieira M.N. and De Felice F.G. (2007). Soluble protein oligomers as emerging toxins in Alzheimer's and other amyloid diseases. IUBMB life 59 (4–5): 332–45. doi:10.1080/15216540701283882. PMID 17505973.

[11] Gebauer, D. and Völkel, A. and Cölfen, H. (2008). Stable prenucleation calcium carbonate clusters. Science 322 5909: 1819–1822.

[12] Gebauer, D. and Cölfen, H.(2011). Prenucleation clusters and non-classical nucleation.Nano Today 6 6: 564–584.

[13] Gambini I. and Vuillon L., An algorithm for deciding if a polyomino tiles the plane, *Theoretical Informatics and Applications*, vol. 41, 2 (2007), 147–155.

[14] Gambini I. and Vuillon L., How many faces can polycubes of lattice tilings by translation of $\mathbb{R}^3$ have?, *the electronic journal of combinatorics*, Vol 18, (2011), P199.

[15] Gambini I. and Vuillon L., Non lattice periodic tilings of $\mathbb{R}^3$ by single polycubes, *Theoretical Computer Science*, 432, (2012), 52–57.

[16] Golomb S. W., Checker boards and polyominoes, *Amer. Math. Monthly*, vol. 61, 10 (1954) 675–682.

[17] Goodsell, D.S. and Olson, A.J. 2000. Structural symmetry and protein function. Annu. Rev. Biophys. Biomol. Struct. 29: 105–153.

[18] Grunbaum B. and Shephard G.C., Tilings with congruent tiles, *Bull. Amer. Maths. Soc.*, vol 3, 3 (1980) 951–974.

[19] Haataja L, Gurlo T, Huang CJ, Butler PC (May 2008). "Islet amyloid in type 2 diabetes, and the toxic oligomer hypothesis". Endocrine Reviews 29 (3): 303–16. doi:10.1210/er.2007-0037. PMC 2528855. PMID 18314421.

[20] Höppener J.W., Ahrèn B. and Lips C.J. (August 2000). "Islet amyloid and type 2 diabetes mellitus". The New England Journal of Medicine 343 (6): 411–9. doi:10.1056/NEJM200008103430607. PMID 10933741.

[21] Irvine G.B., El-Agnaf O.M., Shankar G.M. and Walsh D.M. (2008). "Protein aggregation in the brain: the molecular basis for Alzheimer's and Parkinson's diseases". Molecular

medicine (Cambridge, Mass.) 14 (7–8):   451–64.   doi:10.2119/2007-00100.Irvine.
PMC 2274891. PMID 18368143.

[22] Janin J., Bahadur R.P. and Chakrabarti P. Protein-protein interaction and quaternary structure. Q Rev Biophys 2008;41(2):133–80.

[23] LaBean T. and Park S. H. (2006). Self-assembled DNA Nanotubes. Nanotechnologies for the Life Sciences.

[24] Levy E.D. and Teichmann S., Structural, Evolutionary, and Assembly Principles of Protein Oligomerization. In Jesús Giraldo and Francisco Ciruela, editors: Progress in Molecular Biology and Translational Science, Vol. 117, Burlington: Academic Press, 2013, pp. 25–51.

[25] Liu, Y., Gotte, G., Libonati, M. and Eisenberg, D. (2001) A domain-swapped RNase A dimer with implications for amyloid formation. Nat Struct Biol 8, 211–214.

[26] Lomas D.A. and Carrell R.W. (2002) Serpinopathies and the conformational dementias. Nature Reviews Genetics 3: 759–768.

[27] Lwin, T. Z., Durant, J. J. and Bashford, D. (2007) A fluid salt-bridging cluster and the stabilization of p53. J Mol Biol 373, 1334–1347.

[28] Monod J., Wyman J., and Changeux J.-P. (1965). On the nature of allosteric transitions: a plausible model. J. Mol. Biol. 12: 88–118.

[29] Ochieng J. and Chaudhuri G. (2010) Cystatin superfamily. J Health Care Poor Underserved 21: 51-70.

[30] Protein Data Bank : http://www.rcsb.org/pdb/home/home.do

[31] Senechal, M. (1995) Quasicrystals and geometry, Cambridge University Press.

[32] Swapna L.S., Srikeerthana K. and Srinivasan N. (2012) Extent of Structural Asymmetry in Homodimeric Proteins: Prevalence and Relevance. PLoS ONE 7(5): e36688. doi:10.1371/journal.pone.0036688

[33] Tsitrin Y, Morton CJ, el-Bez C, Paumard P, Velluz MC, et al. (2002) Conversion of a transmembrane to a water-soluble protein complex by a single point mutation. Nat Struct Biol 9: 729-733.

[34] Tuncbag, N., Kar, G., Keskin, O., Gursoy, A., and Nussinov, R. (2009) A survey of available tools and web servers for analysis of protein–protein interactions and interfaces. Briefings in Bioinformatics 10, 217.

[35] Twarock, R., (2006) Mathematical virology: a novel approach to the structure and assembly of viruses. Philosophical Transactions of the Royal Society A: Mathematical, Physical and Engineering Sciences 364, 1849, 3357–3373.

[36] de Vries, S. J., and Bonvin, A. M. (2008) How proteins get in touch: interface prediction in the study of biomolecular complexes. Curr Protein Pept Sci 9, 394-406.

[37] Winfree, E., Liu, F., Wenzler, L. A., and Seeman, N.C., Design and self-assembly of two-dimensional DNA crystals., Nature 1998, 394, 539-544.

[38] Yadid I, Kirshenbaum N, Sharon M, Dym O, Tawfik DS (2010) Metamorphic proteins mediate evolutionary transitions of structure. Proc Natl Acad Sci U S A 107: 7287-7292.

[39] Yin, P., Hariadi, R. F., Sahu, S., Choi, H. M., Park, S. H., LaBean, T. H., and Reif, J. H. (2008). Programming DNA tube circumferences. Science, 321(5890), 824-826.